NASA TECHNICAL MEMORANDUM

NASA TM X-62,164

NASA TM X-62,164

ASPECTS OF INVESTIGATING STOL NOISE USING LARGE-SCALE WIND-TUNNEL MODELS

Michael D. Falarski, David G. Koenig, and Paul T. Soderman

Ames Research Center

and

U.S. Army Air Mobility R&D Laboratory
Moffett Field, Ca. 94035

June 1972

ASPECTS OF INVESTIGATING STOL NOISE USING LARGE-SCALE WIND-TUNNEL MODELS

Michael D. Falarski, David G. Koenig and Paul T. Soderman

Ames Research Center
and
U.S. Army Air Mobility Research & Development Laboratory

SUMMARY

The applicability of the NASA Ames 40- by 80-Foot Wind Tunnel for acoustic research on STOL concepts has been investigated. The acoustic characteristics of the wind tunnel test section has been studied with calibrated acoustic sources. Acoustic characteristics of several large-scale STOL models have been studied both in the free-field and wind tunnel acoustic environments. The results of these studies indicate that the acoustic characteristics of large-scale STOL models can be measured in the wind tunnel if the test section acoustic environment and model acoustic similitude are taken into consideration. The reverberant field of the test section must be determined with an acoustically similar noise source. Directional microphone and extrapolation of near-field data to far-field are some of the techniques being explored as possible solutions to the directivity loss in a reverberant field. The model sound pressure levels must be of sufficient magnitude to be discernable from the wind tunnel background noise.

INTRODUCTION

Acceptance of a commercial STOL aircraft will be very dependent on its ability to operate at low noise levels. The primary reason for this is the close proximity of STOL (short takeoff and landing) ports to areas of high population density. The proposed 95 EDNdB noise limit at 152 m (500 ft) from runway centerline is substantially lower than the existing FAR 36 limits on commercial CTOL aircraft. As the concern over noise pollution grows and STOL operation becomes more widespread, it is quite possible that the acceptable noise level will be reduced even further. Extensive research will have to be conducted to achieve noise reductions throughout the STOL flight regime.

The staff of the Ames 40- by 80-Foot Wind Tunnel has conducted extensive research in STOL aerodynamics (see reference 1). Because of the wind tunnels large size (see figure 1), the models tested incorporate flight-worthy propulsion systems. Aside from the aerodynamic system benefits of this capability, the large-scale models provide realistic acoustic sources. With this equipment available the desirability of acoustic investigation is evident. The development of the wind tunnel as an acoustic research facility permits the analysis of fly over noise long before an aircraft is available. This paper will present the results of work to develop the Ames 40- by 80-Foot Wind Tunnel into an acoustic measurement range.

NOTATION

OASPL	overall sound pressure level, dB ref. .0002 microbar
PNL	perceived noise level, PNdB
PTAUG	augmentor total pressure, cm. hg(in. hg)
q	free-stream dynamic pressure, n/m^2(psf)
SPL	sound pressure level, dB ref. .0002 microbar
V_J	fan exit jet velocity, m/sec (ft/sec)
V_∞	free-stream velocity, m/sec (ft/sec)
δ_f	flap deflection, deg
$\Lambda_{c/4}$	wing sweep at the quarter chord, deg

ACOUSTIC MEASUREMENTS IN THE WIND TUNNEL

The acoustic characteristics of the wind tunnel were investigated with several acoustic sources (see reference 2). These studies have shown that reverberations, background noise levels, and standing waves present problems in measuring free-field noise in the wind tunnel. These problems, as well as possible solutions, will be discussed in this section.

Test Section Reverberation

The acoustic studies have shown the test section to be quite reverberant. This can be seen in the rise above free-field levels of the test section measurements as the microphone is moved away from the source (see figure 2). The test section Hall Radius, which is the distance from the source where the reverberant field and the direct field are equal, is approximately 4.6 m (15 ft). Because of the model shape, location, and size, it is usually not possible to place microphones within the Hall Radius. Therefore, to determine free-field noise levels the data must be corrected for the reverberation. This requires calibration of the wind tunnel with an acoustic source which is similar to the acoustics of the model.

Acoustic directivity.- The major difficulty a reverberant field presents is the masking of directivity. This can be handled by time consuming calibration procedures for broad-band noise. However, other solutions to this problem which are being explored include a directional microphone, a phased array of microphones, and calculation of far-field levels from near-field measurements. An example of the type of directional microphones being investigated is the porous pipe microphone shown in figure 3. The porous pipe allows weak coupling between the acoustic pressures inside and outside the pipe. A ½ inch omnidirectional microphone is located at the end of the porous pipe. The solid cone inside the pipe produces an anechoic termination of all waves except those traveling towards the microphone. In the frequency range for which it is designed the microphone increases the Hall Radius of the wind tunnel to 9.15 m (30 ft). Its use is limited at present because it must be oriented parallel to the wind stream to avoid high wind noise measured when oriented in any other plane (see figure 4). This flow noise can possibly be reduced by designing the porous pipe in the form of a porous strip conformal with the upper and lower surface of an airfoil. The other limiting factor is the microphone length. Its directivity is a function

of its length and to achieve reasonable directivity at 500 Hz, the microphone must be 1.22 m (4 ft) long.

Another possible method of measuring directivity in a reverberant field is an electronically phased array of microphones. The microphones can be arranged in either an end-on array or a broadside array. The end-on array consists of 4 or 5 microphones spaced along a line radiating from the noise source. The broadside array has a row of 4 or 5 microphones spaced along a line parallel to the source. In either case the signals from each microphone are electronically delayed such that the direct signal is reinforced while the wave fronts from reverberation or background sources are cancelled. The frequency response and directivity of the array are a function of the delay time, microphone spacing, and system rigidity.

By taking measurements in the near-field the direct radiated signal is made much larger than the reverberant signal. Far-field levels computed from these near-field measurements offer another solution to the wind tunnel reverberant field problem. This approach is difficult to implement experimentally because of the large number and accuracies of the measurements required. Analyses and experiments are underway to define the experimental problem and devise means of practical implementation.

Acoustic power.- The investigation of the test section inlet and diffuser acoustic environment with a source in the test section, indicates the reverberant field in these two areas is fairly diffuse and that the acoustic energy tends to flow out of the test section. This means that the sound waves are traveling equally in all directions except toward the source and the sound pressure for a given cross section does not vary from point to point due to reflection or interference. This allows the measurement of the total sound power radiated in the test section to be estimated from single measurements of the sound pressure in the inlet and diffuser of the wind tunnel.

Wind Tunnel Background Noise

Operation of the wind tunnel creates a background noise floor, which is established by the noise of the tunnel drive system and wind noise on the microphones. A frequency spectrum of this noise (see figure 5) shows it to be fairly low frequency and dominated by the fan tones and broadband noise at $q > 958$ n/m^2 (20 psf). At $q < 958$ n/m^2 (20 psf) the fan motor-generator noise is no longer negligible. It consists of three tones at 125, 250, and 500 Hz, which do not vary in frequency with tunnel speed.

The overall level of the noise floor increases with forward speed as is shown in figure 6. The acoustic source being investigated must be sufficiently loud and have a frequency spectrum such that its sound levels are discernible from the background noise. At present this is not a significant problem, but it will be in the future when acoustically treated models having lower noise levels are studied. Because of the large size of the test section and the dominant low frequencies, any significant reduction in the noise floor with acoustic treatment of the wind tunnel is quite difficult. The solutions for the reverberant field problem are also directly applicable to the background noise problem in that they allow discrimination between the noise sources in the test section.

Placing a microphone in a moving air stream creates local turbulence which the microphone senses as radiated acoustic pressures. This contributes a high frequency sound to the background noise floor. While this is not a problem with existing models, future quiet propulsion systems will approach this noise floor. At present aerodynamically shaped nose cones, which substantially diminish the response to turbulence while having little effect on the microphones acoustic properties, are mounted on microphones used in the wind tunnel. Different types of fairings are being studied experimentally to reduce this wind noise even further.

Acoustic Focusing

Reverberant enclosures such as the wind tunnel test section will reflect and focus sound, creating standing waves. To study this phenomenon an optical model of the wind tunnel test section was constructed. The internal surface of the model was covered with a highly reflective foil. A small light source was placed in the center to simulate an acoustic source. The results of the experiment are shown in figure 7. Planes and areas of acoustic focusing were found in the model. These are areas in the wind tunnel which should be avoided. Because this experiment simulated sources of very high frequency or sound after several reflections, further studies must be conducted with more representative acoustic sources to completely understand this problem.

Other Considerations

All extraneous noise sources on the models must be suppressed if their levels are less than 10 dB below the source of interest and their frequency spectrum is coincident with the model source of interest. This is the case with an internally-blown flap (IBF) model such as the augmentor wing, where the high pressure air is provided by an internal air compressor which masks the noise of the augmentor. During a recent test of the augmentor wing model, the compressor inlet noise was suppressed with acoustically lined inlets (see figure 8). In an externally-blown flap (EBF) model a turbofan engine, which provides a good aerodynamic simulation, may not be acceptable for an acoustic simulation. The internal engine noise is very much a function of the engine design. It may have to be suppressed with an acoustically treated tail pipe to allow investigation of jet scrubbing noise.

As discussed previously, the model noise must be of sufficient amplitude to be discernable from the wind tunnel background noise. This can be accomplished by mounting the microphones closer to the model, although not close enough to be in the acoustic near-field.

TESTS

To gain more understanding of the wind tunnel acoustic environment, several models were investigated both in the free-field and in the wind tunnel. The configurations listed below will be discussed (the aerodynamic and acoustic characteristics of the models are presented in references 3 thru 8):

1. Lift fan semispan wing
2. OV-10 rotating cylinder flap aircraft
3. Externally-blown jet flap semispan wing
4. Swept augmentor wing-internal flow jet flap model

For the first three tests, wind tunnel reverberation corrections were derived from the point source calibration of the test section reported in reference 2. For all the tests, ½ inch B. and K. omnidirectional condenser microphones, equipped with windshield nose cones, were used to measure the sound pressure levels.

RESULTS AND DISCUSSION

Lift Fan Semispan Wing

This configuration was a swept, tapered semispan wing with a single, .93 m (3 ft) diameter, 1.3 pressure ratio, lift fan mounted in the wing. The model installed in the wind tunnel is shown in figure 9. The geometric details of the wing are presented in figure 10. The fan was tip driven by the exhaust gas of a J-85 turbo jet with an acoustically treated inlet to suppress the engine compressor noise. A free-field investigation was made with the isolated fan. The results of this study were corrected for ground and atmospheric attenuation. As can be seen in figure 11, the sound pressure level and directivity at the blade passage frequency for the free-field and wind tunnel studies show good agreement except for the 20° near the plane of the fan. The lower noise in that direction is contrary to expectations because the reverberant field would increase noise; however, the wind tunnel model had a relatively large chord surface in the plane of the fan which may have reduced the inlet to exhaust noise propagation.

OV-10A Rotating Cylinder Flap STOL Aircraft

An OV-10A aircraft has been modified to incorporate a rotating cylinder flap. Geometric details of the flight test vehicle and the flap are presented in figure 12. The rotating cylinder located at the wing-flap junction induces flow over the flap, creating high circulation lift. The aircraft noise was measured both in actual flyover tests as well as in the wind tunnel. The wind tunnel data was corrected for reverberation and the flyover data was adjusted for ground reflection and ground and atmospheric attenuation. The one-third octave band frequency spectrums of the two studies are compared in Figure 13. The agreement is very good, although the wind tunnel levels tend to be slightly lower than the flight results. There is also no tone at the 100 Hz blade passage frequency in the flight data. This may be due to the 1/8 of a second sampling time for the flight test data analysis.

Externally-Blown Jet Flap Semispan Wing

The externally-blown jet flap model is shown installed in the wind tunnel in figure 14. The microphones were mounted in the plane of the fan on a 6.1 m (20 ft) semicircle. The geometric details of the model are also presented in figure 14. The .76 m (30 in) diameter, 1.03 pressure ratio, ducted fan is mounted below the wing so that its slipstream impinges on the large chord flap system. Because the model could not be tested in free-field, it was installed in a large, enclosed preparation area. The acoustic response of this area was calibrated using the dodecahedron acoustic source described in reference 2. It proved to be much less reverberant at higher frequencies than the wind tunnel, as can be seen in figure 15. The results of the two independent tests show good agreement. As shown in figure 16, the perceived noise levels agree within 1 PNdB and there is no significant loss in directivity. The sound frequency spectrums compare favorably above 500 Hz (see figure 17). Below 500 Hz the wind tunnel sound pressure levels are 2-3 dB above those of the static test. This is only partially due to the wind tunnel background noise.

Swept Augmentor Wing

The augmentor flap is a form of internally-blown flap incorporating an ejector system. Through a cooperative program with the Canadian Defense Research Council and DeHavilland Aircraft of Canada, Ltd., the aerodynamic and acoustic characteristics of a swept augmentor wing model are being investigated. The model is shown installed in the wind tunnel in figure 18. The augmentor geometry is described in figure 19.

For the acoustic investigation, the inlets of the air compressor which provides the high pressure primary air and the tail pipes that exhausted surplus air from the compressor were equipped with sound suppressors. This eliminated the inlet tones and reduced the frequency of the tail pipe noise, thus making the augmentor flap the dominant acoustic source.

The augmentor wing model is a much more distributed acoustic source than any of the previously discussed models, and there was some reservation about the applicability of the previously described point source calibrations. Therefore, reverberation corrections were derived from a comparison of the free-field and wind tunnel data for the take-off flap

setting at several power settings. As indicated in figure 20, there is a significant difference between the two results, especially in the high frequency range. Above 500 Hz the point source shows a correction of 6 dB, while the actual data would indicate little or no correction. Also, the omnidirectional point source calibration indicates that, for the same distance from the source, the reverberation is not a function of location in the test section. This is not the case with the augmentor wing, which shows large variations in reverberation in the middle frequency range with location.

The reverberation corrections derived from the test comparison were applied to the other flap and power settings. Deflecting the flap to the landing configuration changes the acoustic directivity, but the corrections are still applicable as indicated by the close agreement in figure 21. This is also true of the frequency spectrum presented in figure 22.

This data was scaled to a 91,000 Kilogram (200,000 pound) gross weight aircraft. This can be done simply and accurately by operating the model at full scale values of jet flow (total pressure and temperature). The acoustic scale factor is then the square root of the nozzle area ratio. The full scale distance is the product of actual measurement distance and the scale factor and the frequency is reduced by the scale factor.

The results of the augmentor wing investigation leads to the conclusion that the point source calibrations are not adequate for correcting acoustic measurements from a large diffused noise source. An investigation of a 3-dimensional externally-blown jet flap model is planned for the near future. This will also be tested in free-field and the wind tunnel. The reverberation field determined from this test will be compared with the augmentor wing results. From this comparison it is hoped that some general guidelines for formulating reverberant field corrections can be determined.

CONCLUDING REMARKS

The results of several model investigations indicate that the acoustic characteristics of STOL models can be measured in the Ames 40- by 80-Foot Wind Tunnel if the test section acoustic environment and model acoustic similitude are taken into consideration. The test section reverberant field must be determined with an acoustically similar noise source. Directional microphones, phased microphone arrays, and the calculations of far-field noise from the far-field measurements are being explored as possible solutions to the problem of measuring directional noise sources in a reverberant field. The model source pressure levels must be of sufficient magnitude to be discernible from the wind tunnel background noise.

REFERENCES

1. Anon: Conference on V/STOL and STOL Aircraft. NASA SP-116, 1966.

2. Bies, David Alan: Investigation of Making Model Acoustic Measurements in the NASA Ames 40- by 80-Foot Wind Tunnel. NASA CR-114352, 1971.

3. Kirk, Jerry V., Hall, Leo P., and Hodder, Brent K.: Aerodynamics of Lift Fan V/STOL Aircraft. NASA TMX-62086, 1971.

4. Kazin, S. B., and Volk, L. J.: LF-336 Lift Fan Modification and Acoustic Test Program. NASA CR-1934, 1971.

5. Weiberg, James A., and Gamse, Berl: Large-Scale Wind Tunnel Tests of an Airplane Model with Two Propellers and Rotating Cylinder Flaps. NASA TND-4489, 1968.

6. Falarski, Michael D., and Aiken, Thomas N.: Large-Scale Wind-Tunnel Investigation of a Semispan Wing Equipped with an Externally-Blown Jet Flap. NASA TMX-62079, 1971.

7. Falarski, Michael D.: Large-Scale Wind-Tunnel Investigation of the Noise Characteristics of a Semispan Wing Equipped with an Externally-Blown Jet Flap. NASA TMX-621

8. Falarski, Michael D., and Koenig, David G.: Aerodynamic Characteristics of a Large-Scale Model with a Swept Wing and Augmented Jet Flap. NASA TMX-62029, 1971.

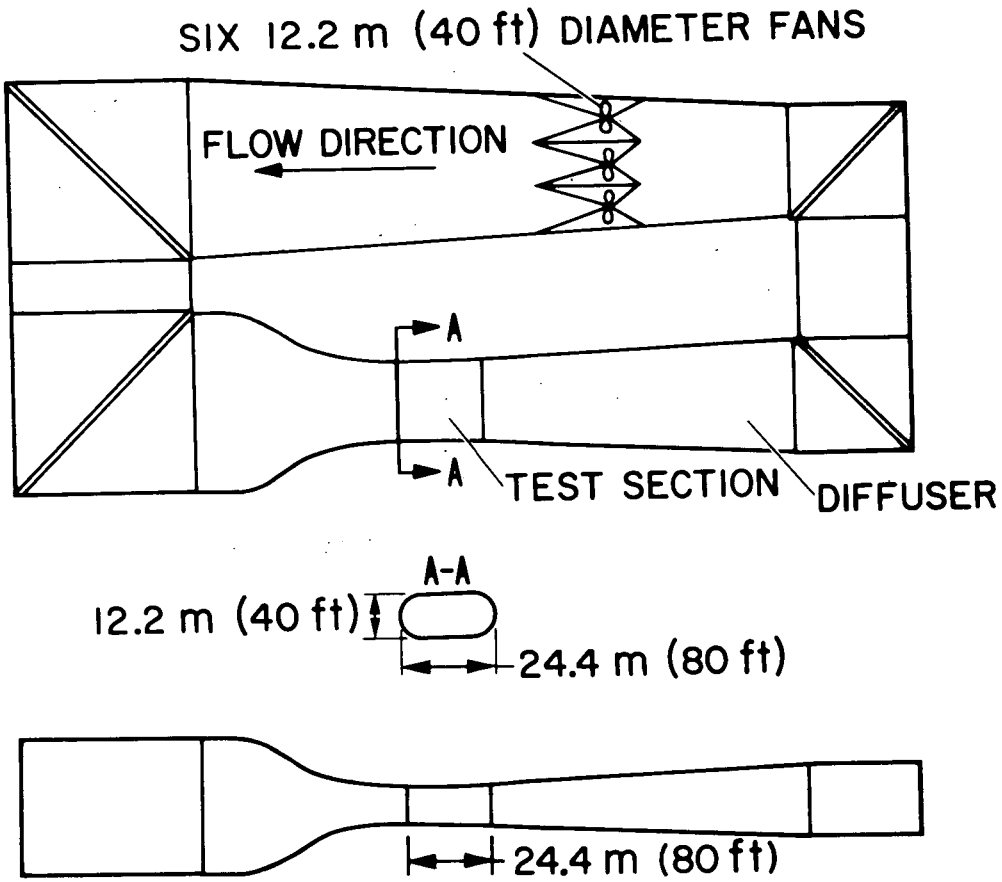

Figure 1.- Geometric details of the NASA Ames 40- by 80-Foot Wind Tunnel.

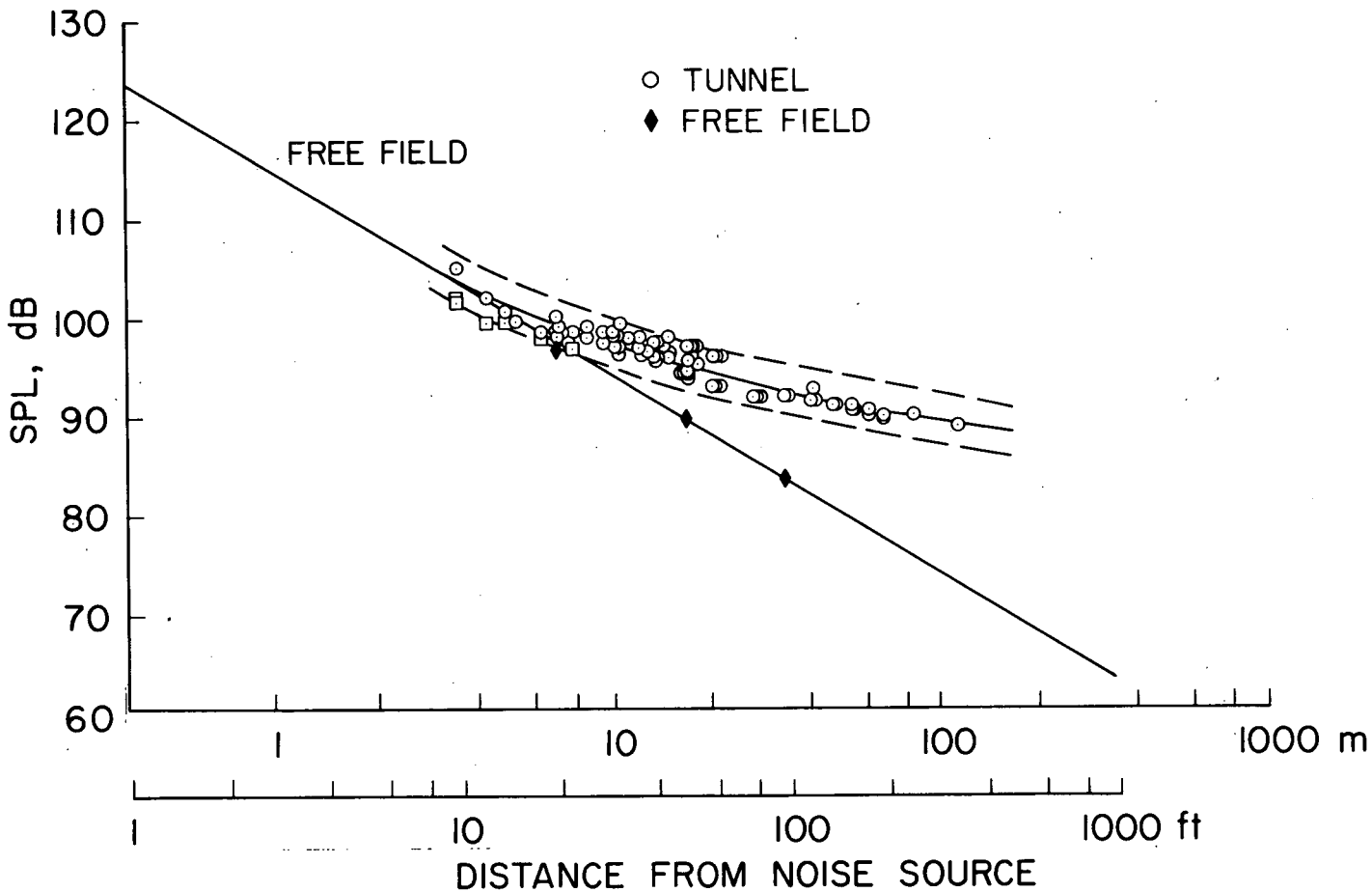

Figure 2.- Variation in overall sound pressure level as a function of distance from a point white noise source in test section.

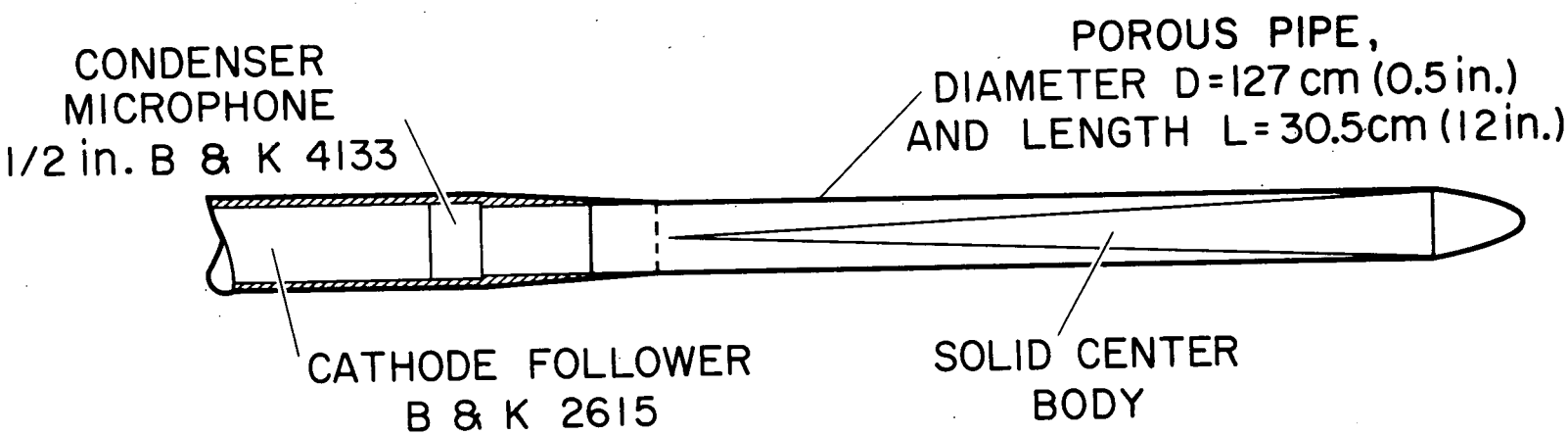

Figure 3.- Cross section of the porous pipe microphone.

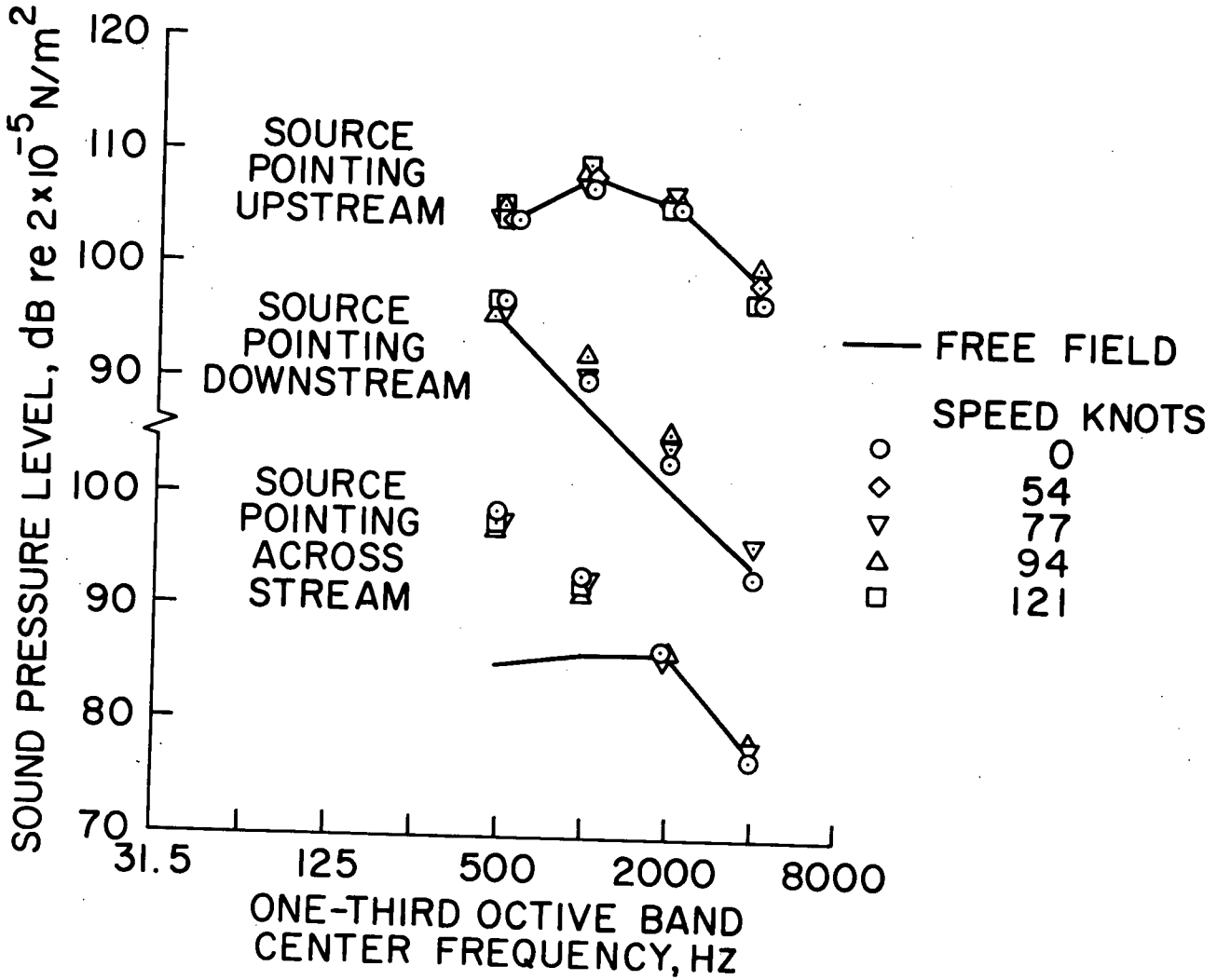

Figure 4.- Porous pipe microphone measurements of sound radiated by a directional source with the wind tunnel operating.

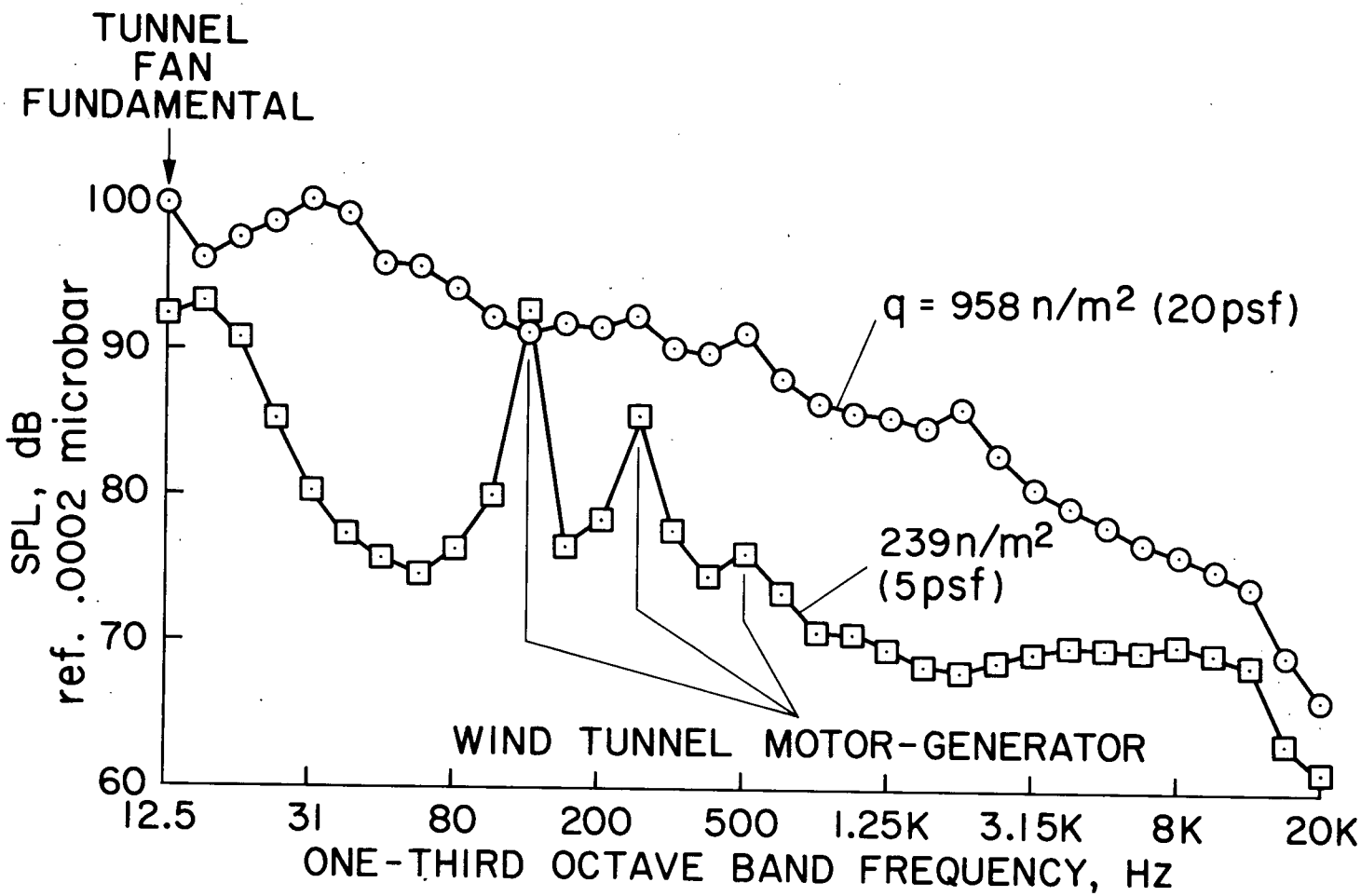

Figure 5.- One-third octave band frequency spectrum of the wind tunnel test section background noise.

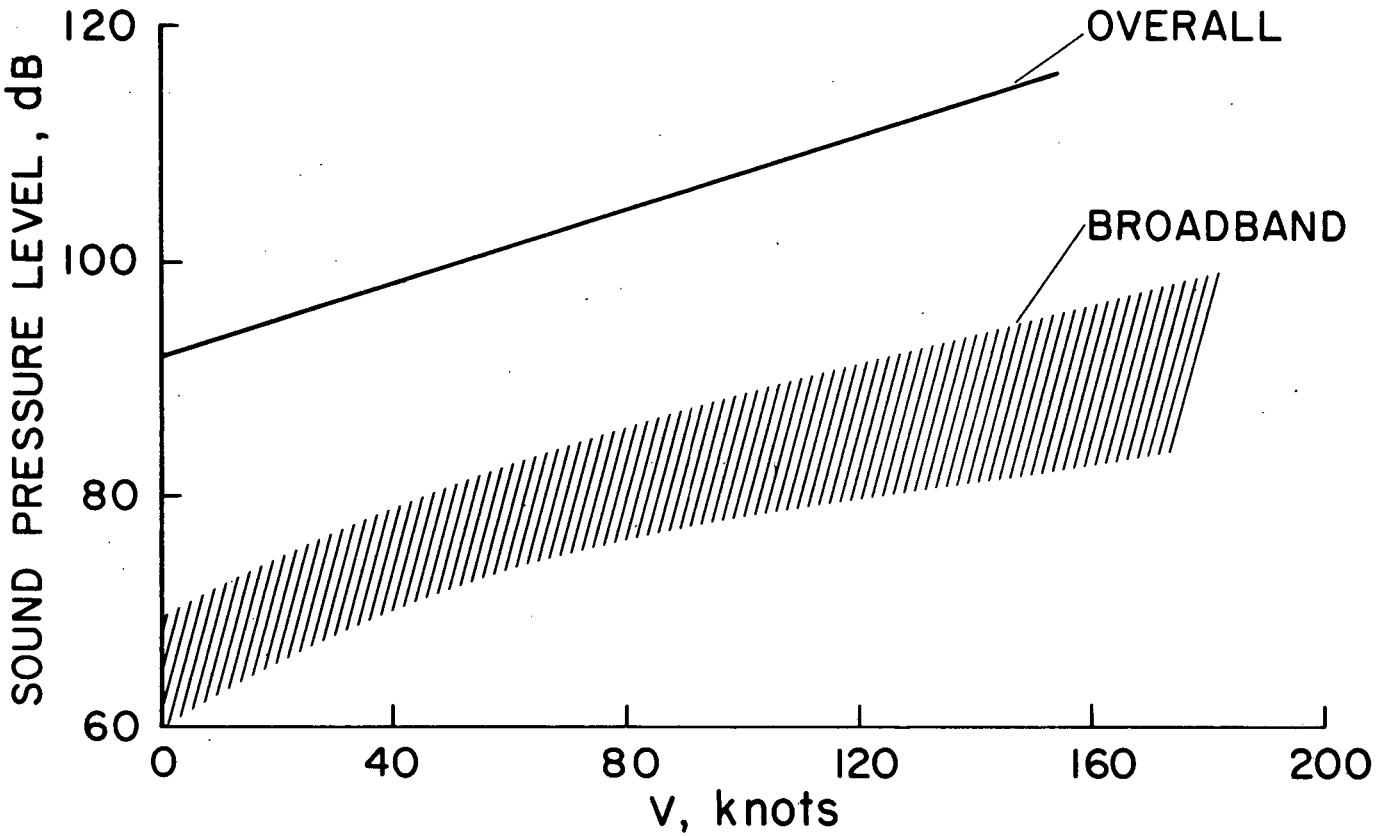

Figure 6.- Variation of the wind tunnel background noise with free-stream velocity.

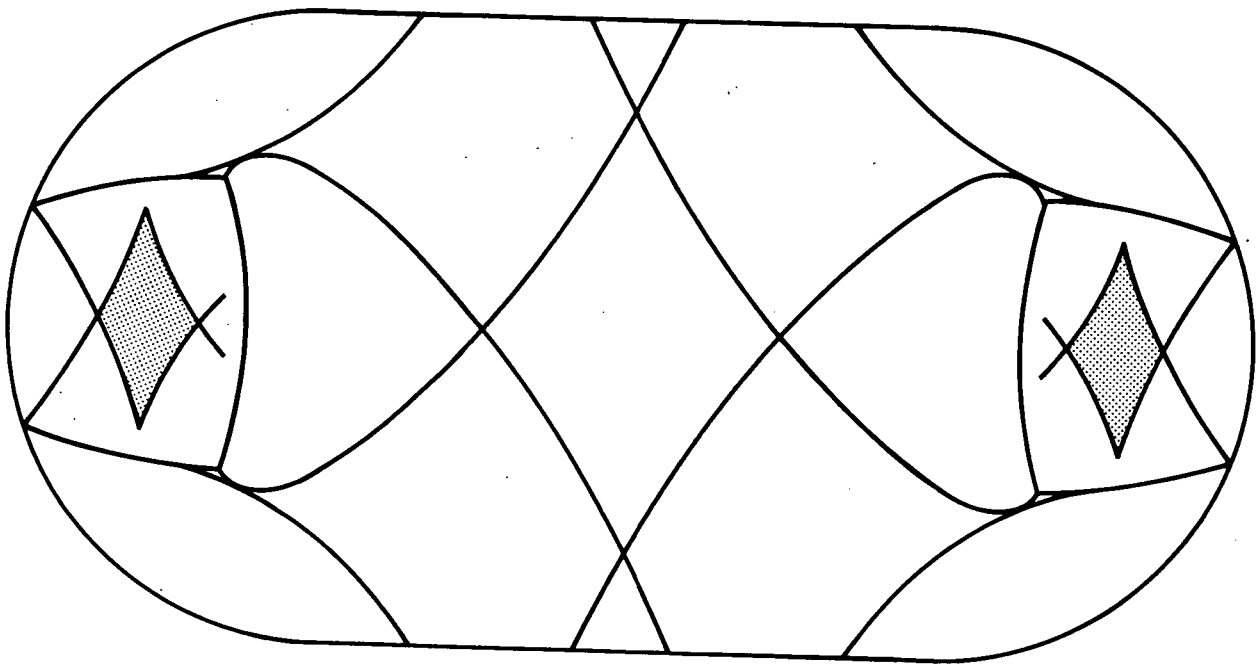

Figure 7.- Optical model map of intense focusing at the end of the test section; distance to the source=12.2m (40 ft).

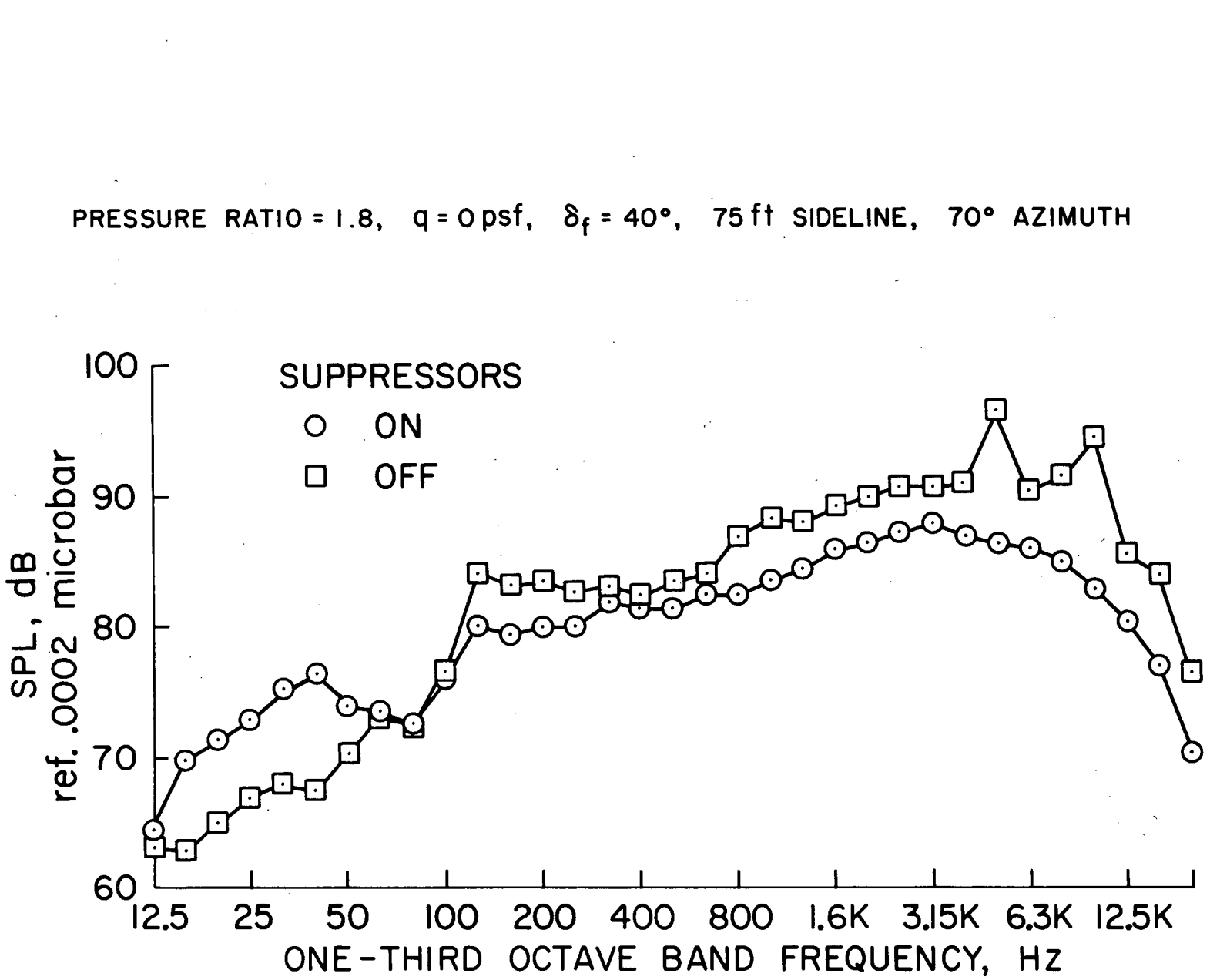

Figure 8.- Suppression of augmentor wing internal compressor inlet noise with acoustically lined inlets.

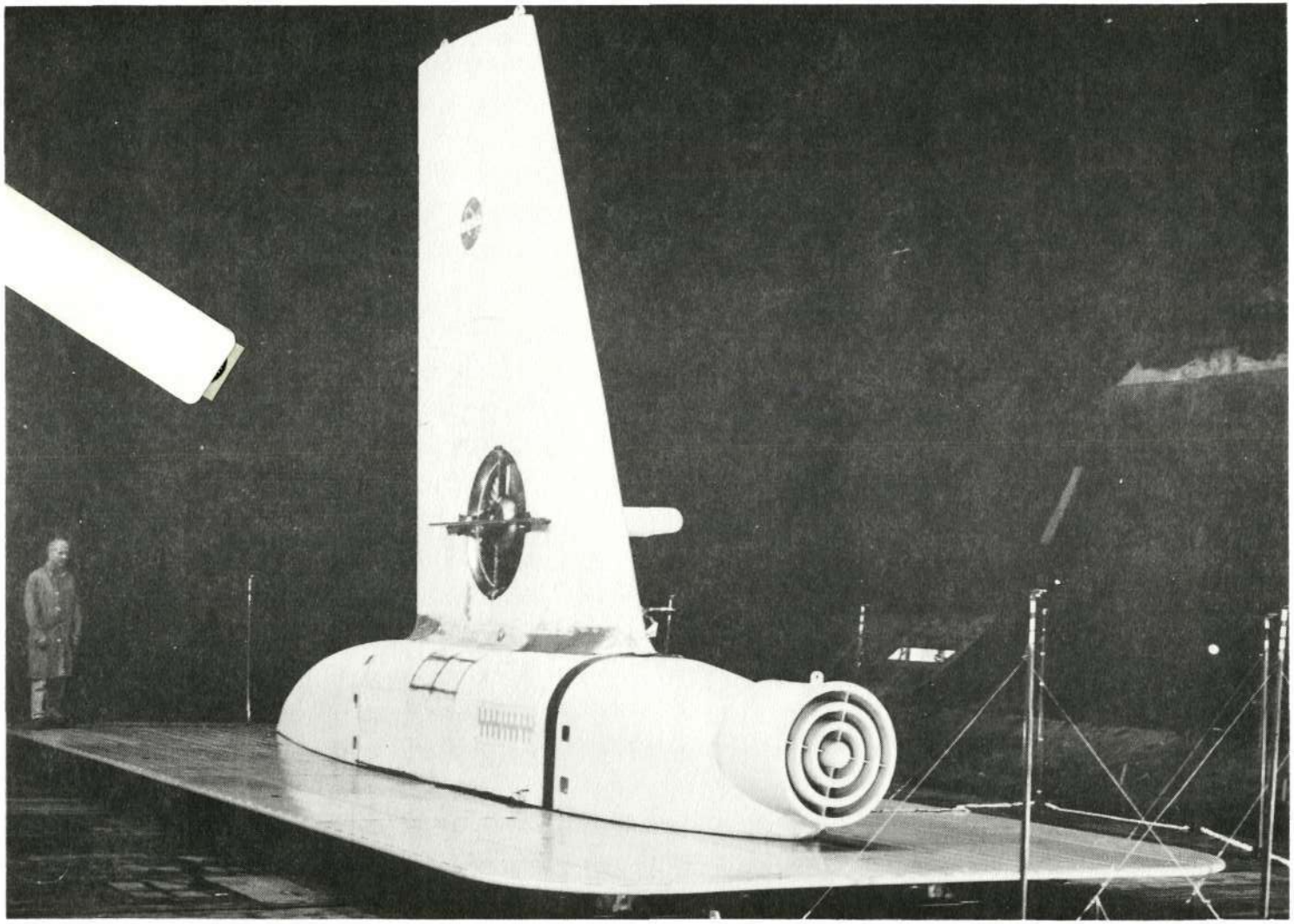

Figure 9.- Installation of the lift fan semispan model in the wind tunnel.

WING AREA 17.95 m^2 (193 ft^2)
ASPECT RATIO 7.36
TAPER RATIO 0.45
AIRFOIL SECTION 65A-211
$A_{C/4}$ = 20 deg

ALL DIMENSIONS IN METERS (FEET)
UNLESS OTHERWISE NOTED

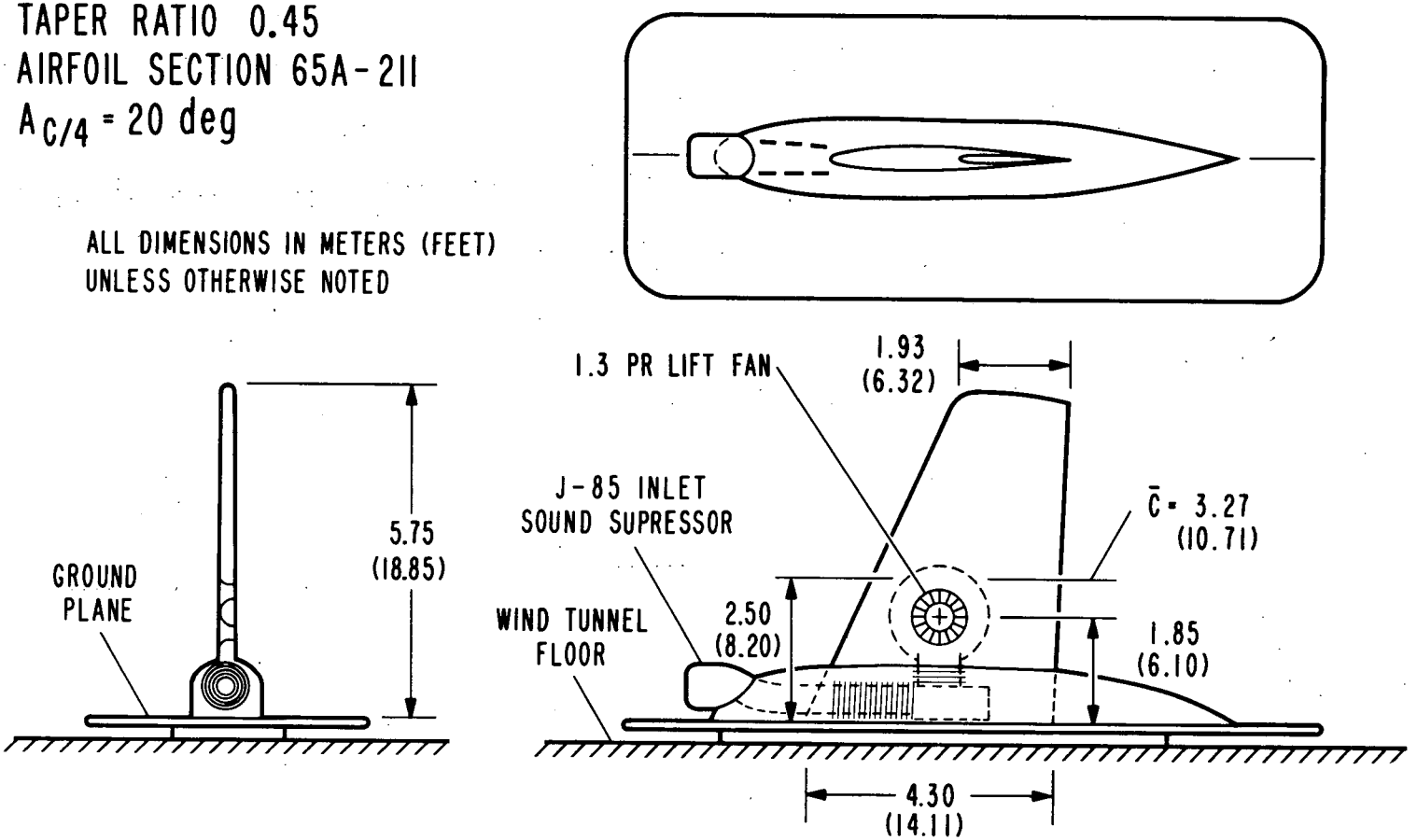

Figure 10.- Geometric details of the lift fan semispan model.

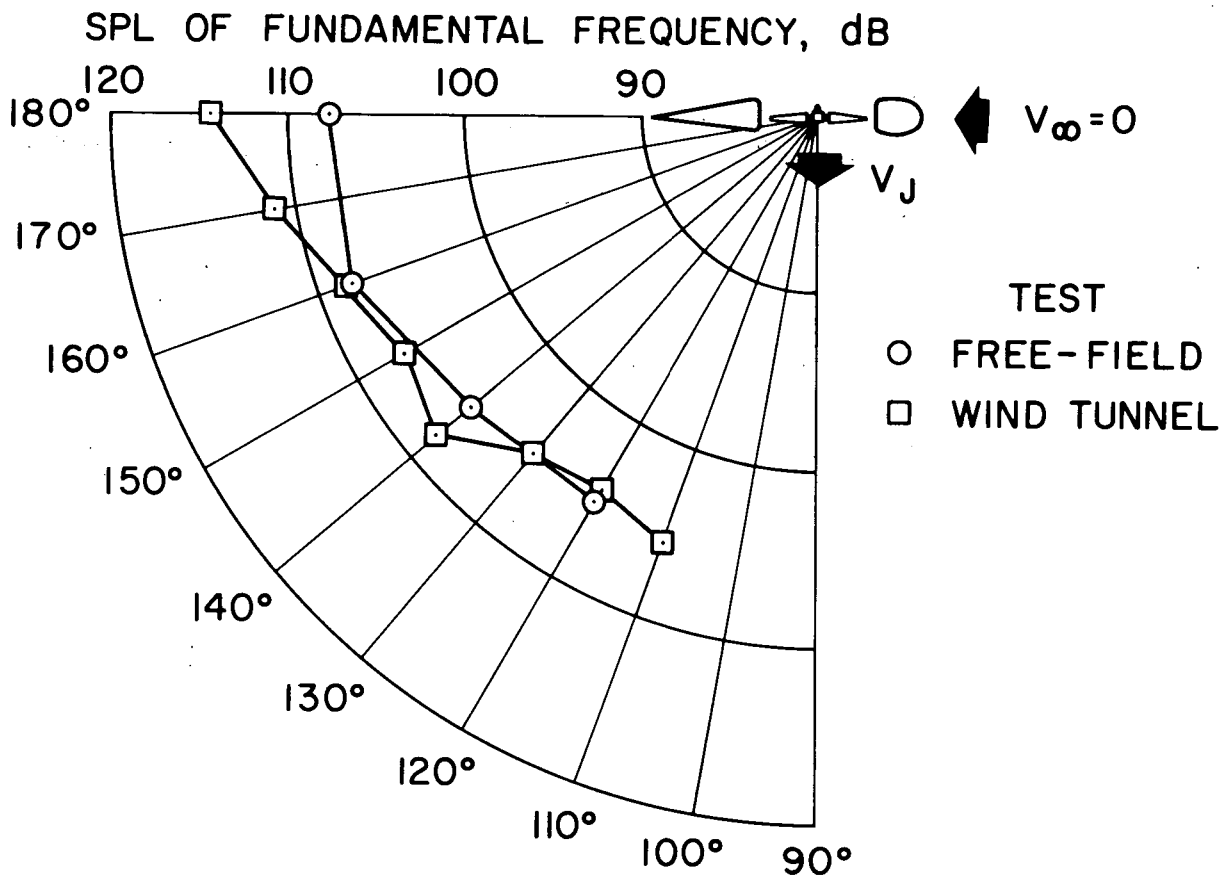

Figure 11.- Comparison of free-field and wind tunnel sound pressure level of the fundamental blade passage frequency of the lift fan semispan model; q=0psf, fan RPM=5260.

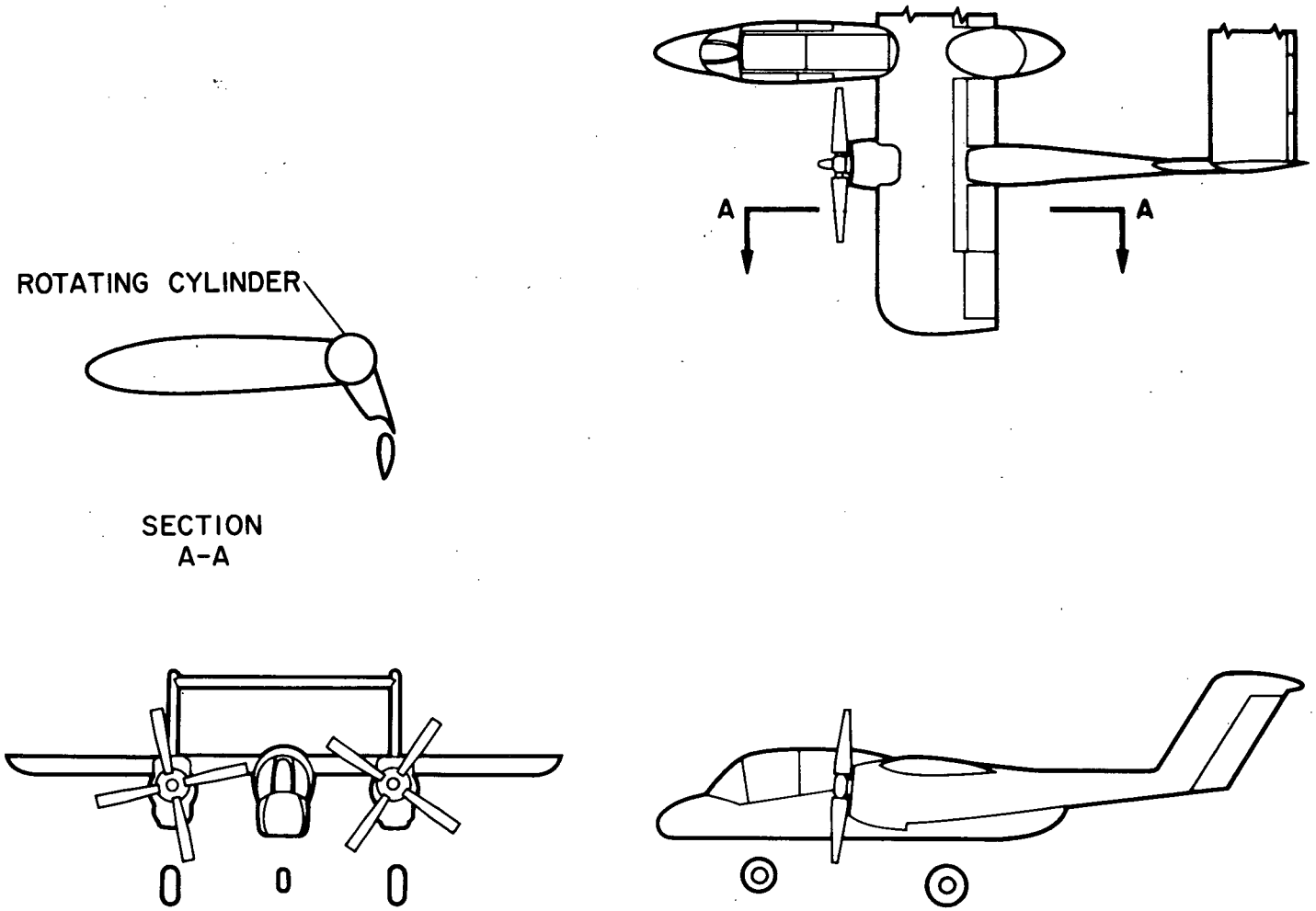

Figure 12.- Geometry of the OV-10A rotating cylinder flap aircraft.

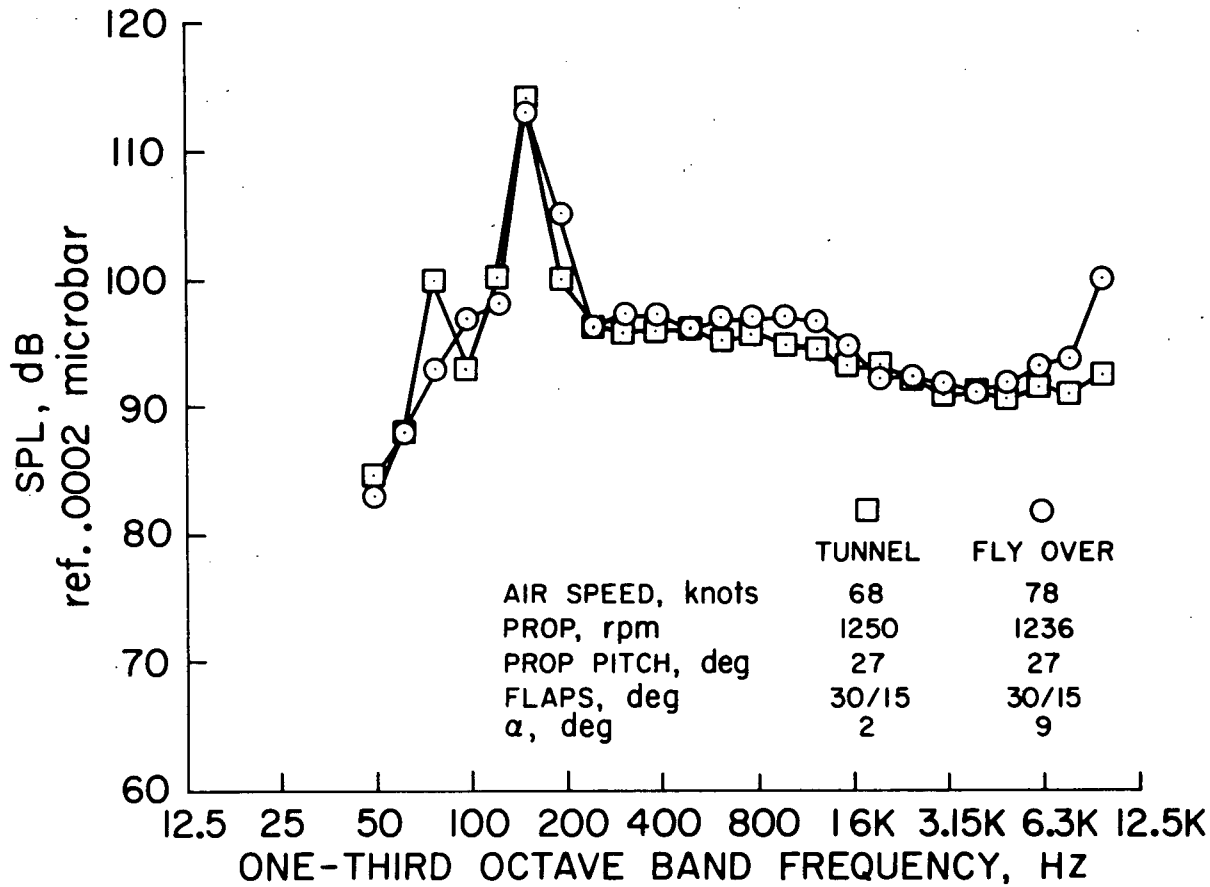

Figure 13.- Comparison of flyover and wind tunnel one-third octave band frequency spectrums of the OV-10A rotating cylinder flap aircraft; air speed=73kts, prop. RPM=1240, prop pitch=27°, flap deflection=30/15°, angle of attack=5 .

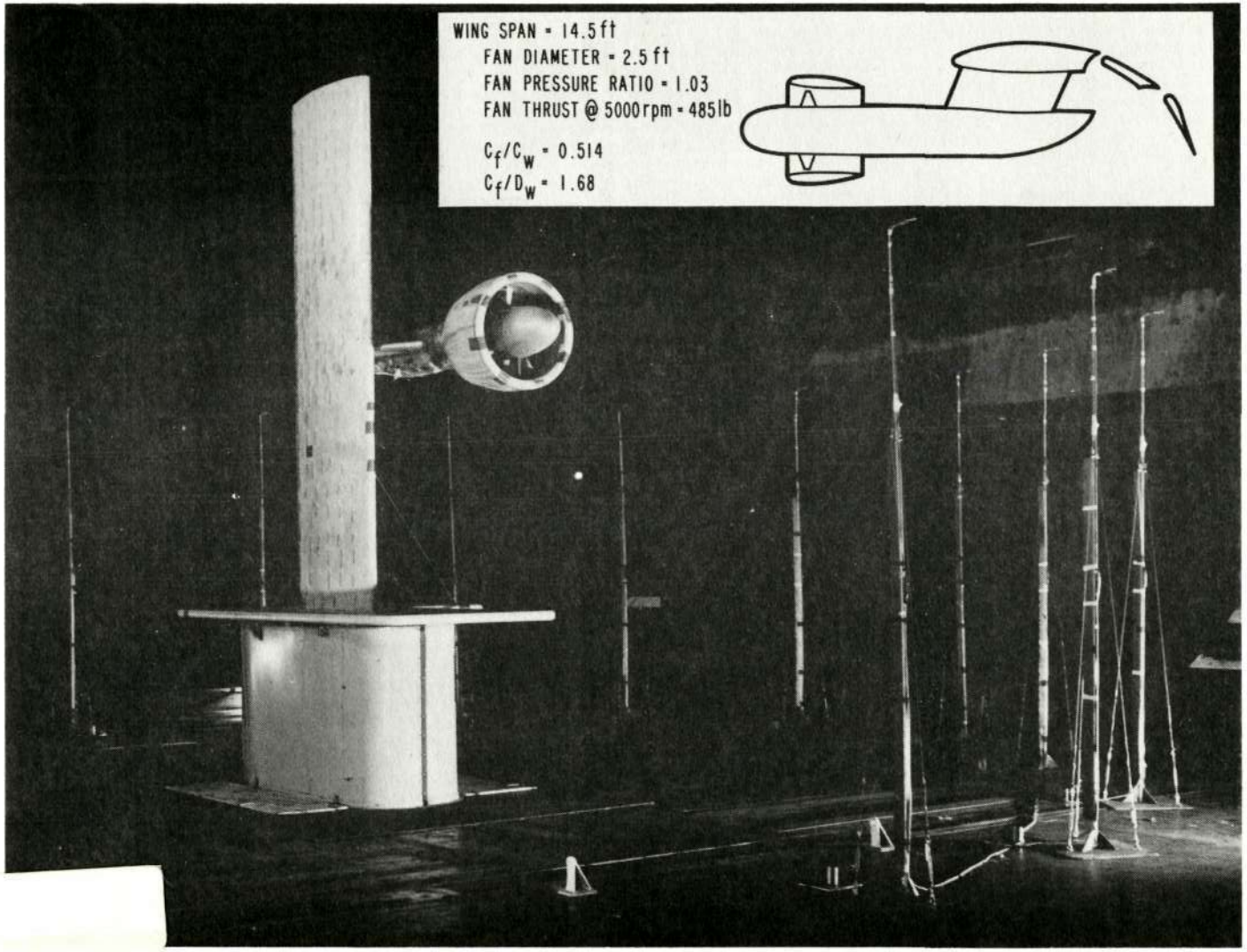

Figure 14.- Installation in the wind tunnel and geometric details of the externally-blown jet flap semispan wing.

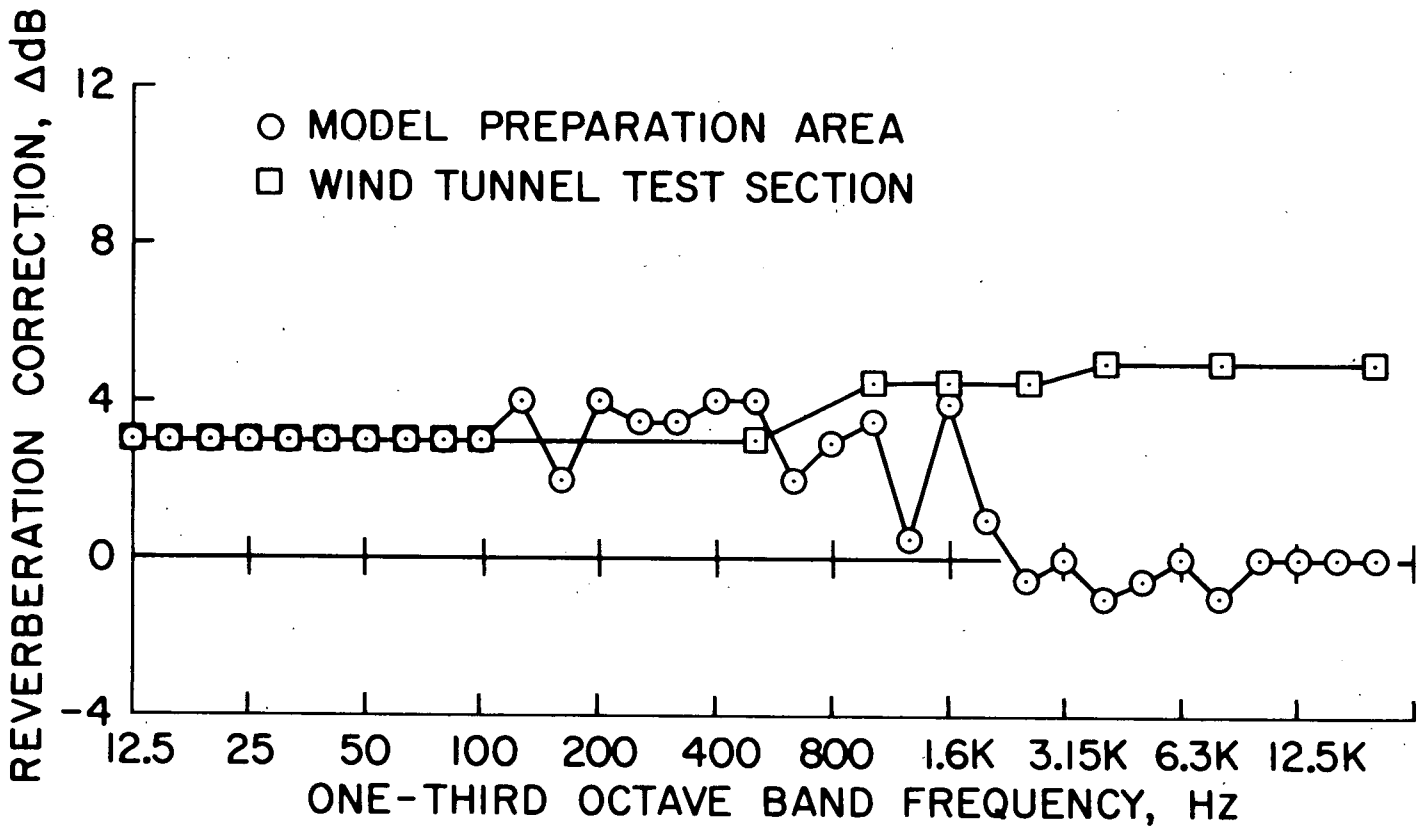

Figure 15.- Wind tunnel and model preparation area reverberation corrections for the EBF semispan wing.

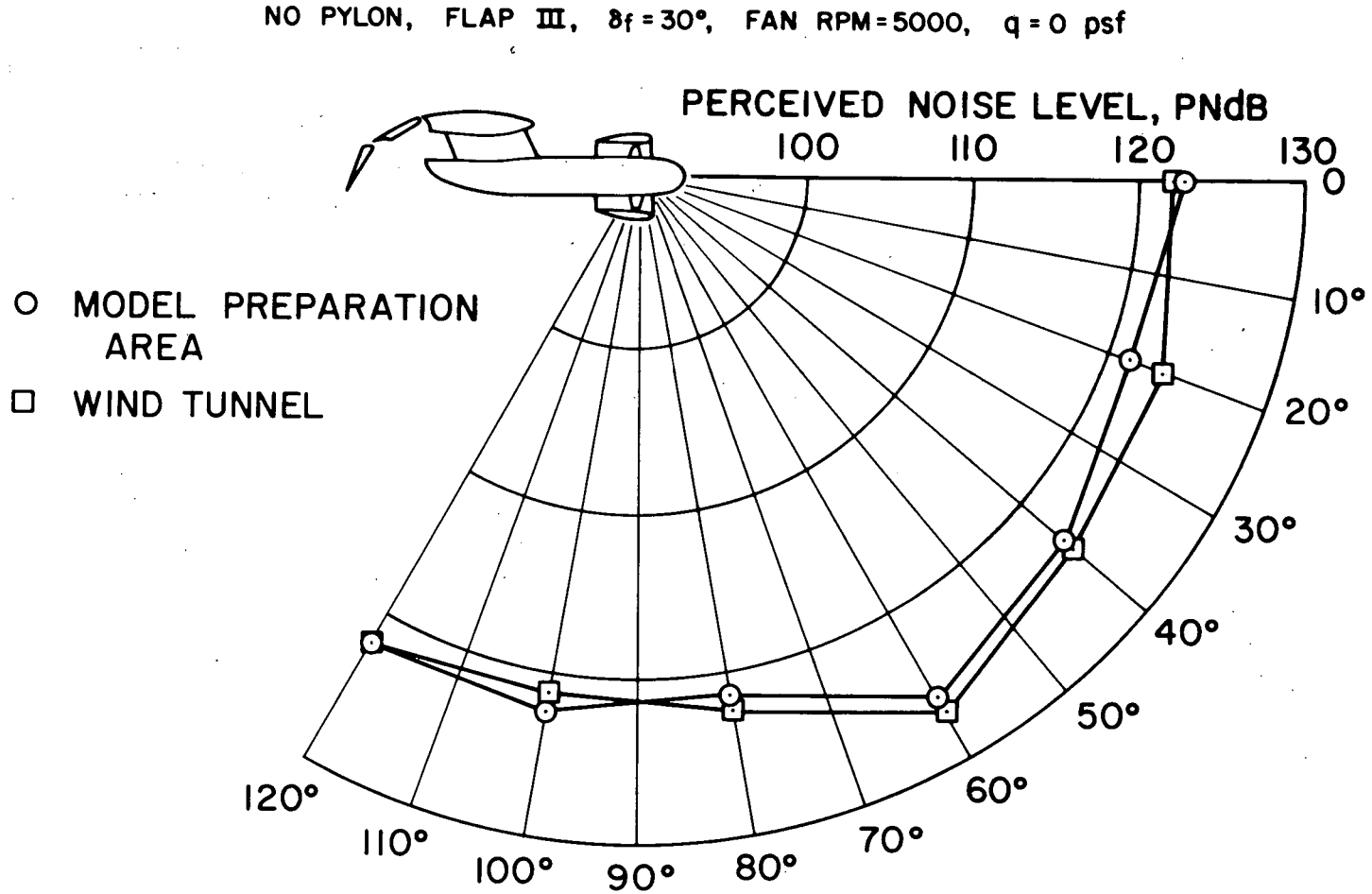

Figure 16.- Comparison of the perceived noise level directivity patterns of the EBF semispan wing in the wind tunnel and model preparation area; q=0psf, flap II, $\delta_f = 30°$, no pylon, 60° azimuth.

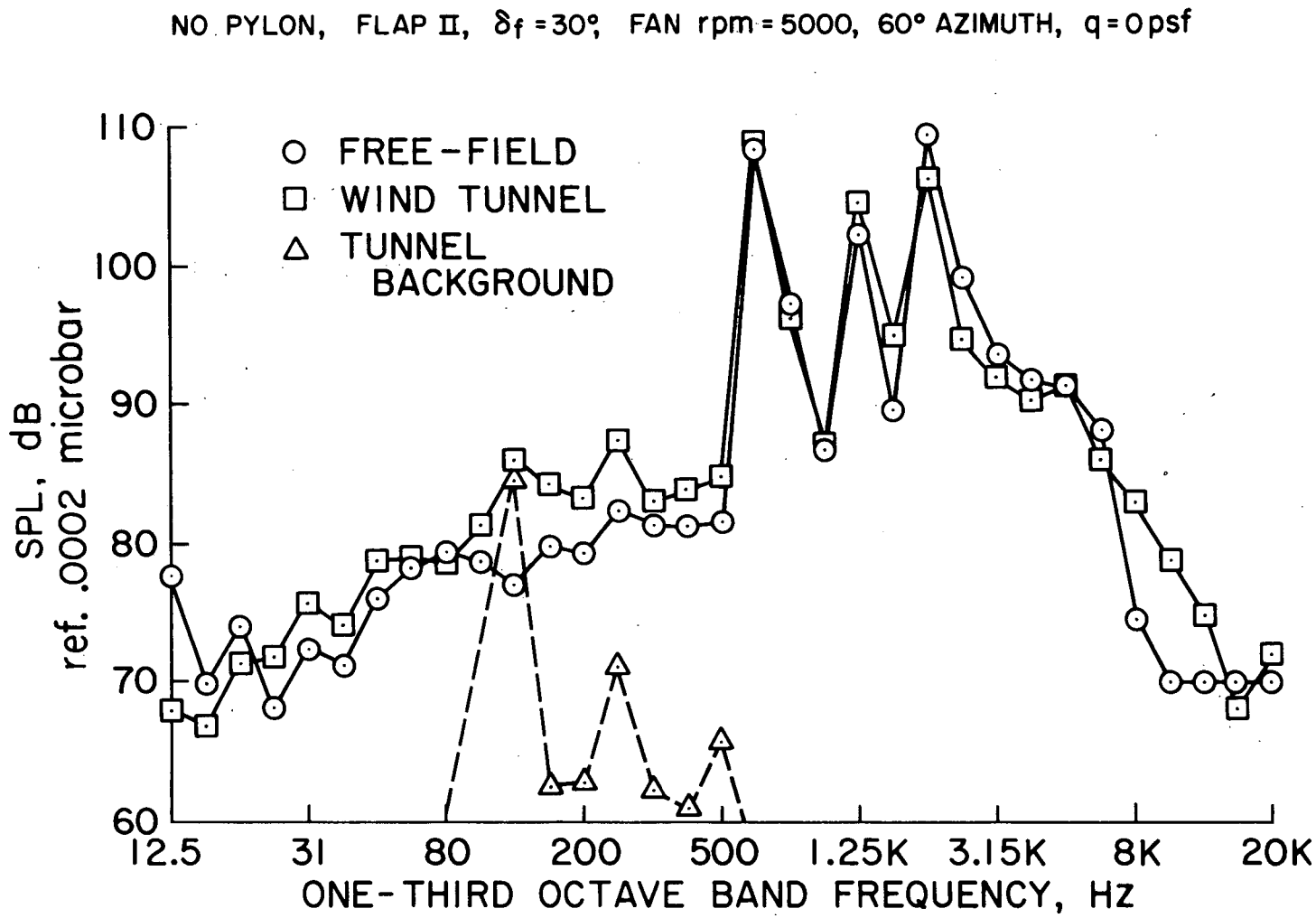

Figure 17.- Comparison of the one-third octave band frequency spectrum of the EBF semispan wing in the wind tunnel and model preparation area; q=0psf, flap II, δ_f= 30°, no pylon, 60° azimuth.

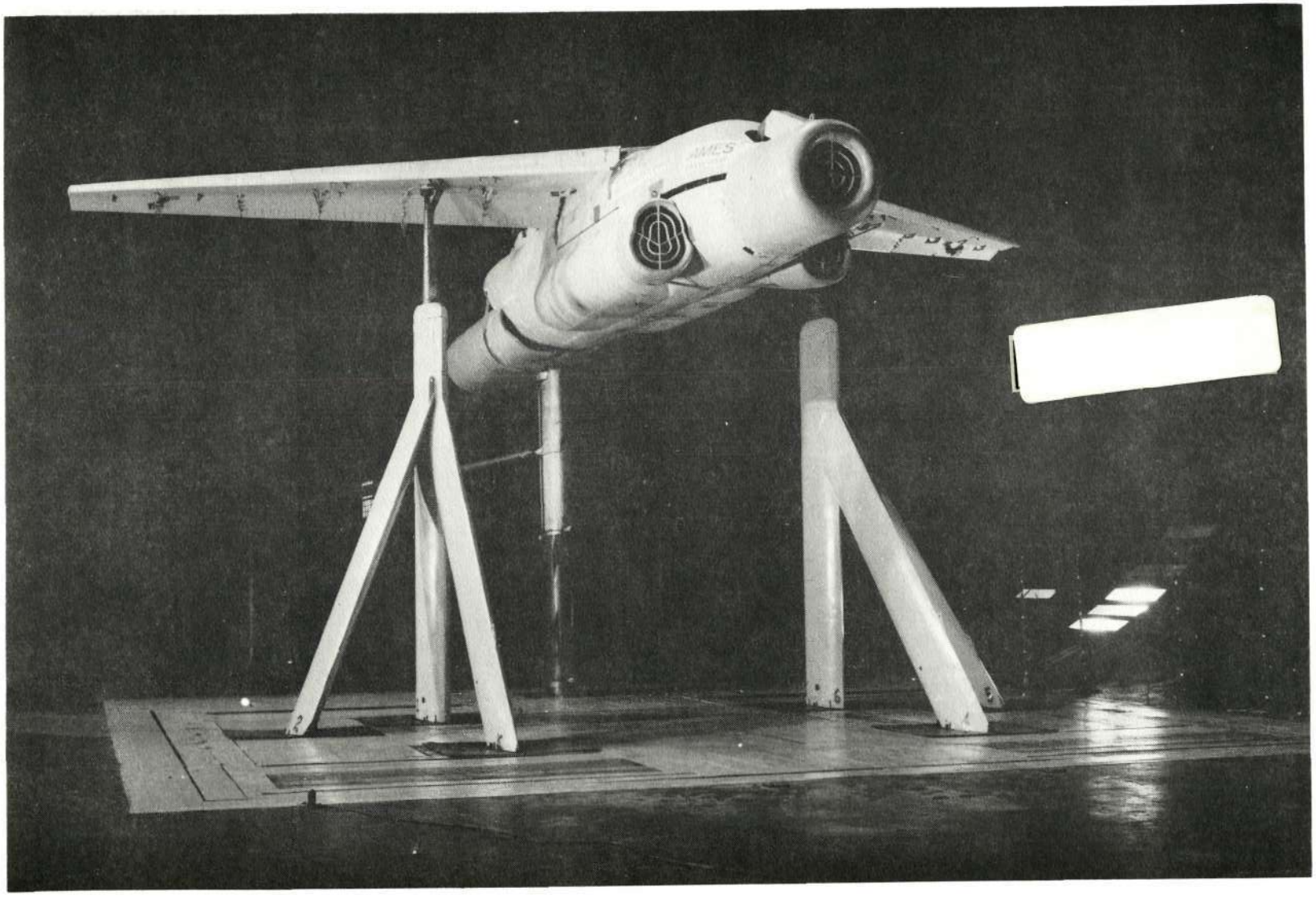

Figure 18.- Installation of the swept augmentor wing model in the wind tunnel with compressor inlet sound suppressors.

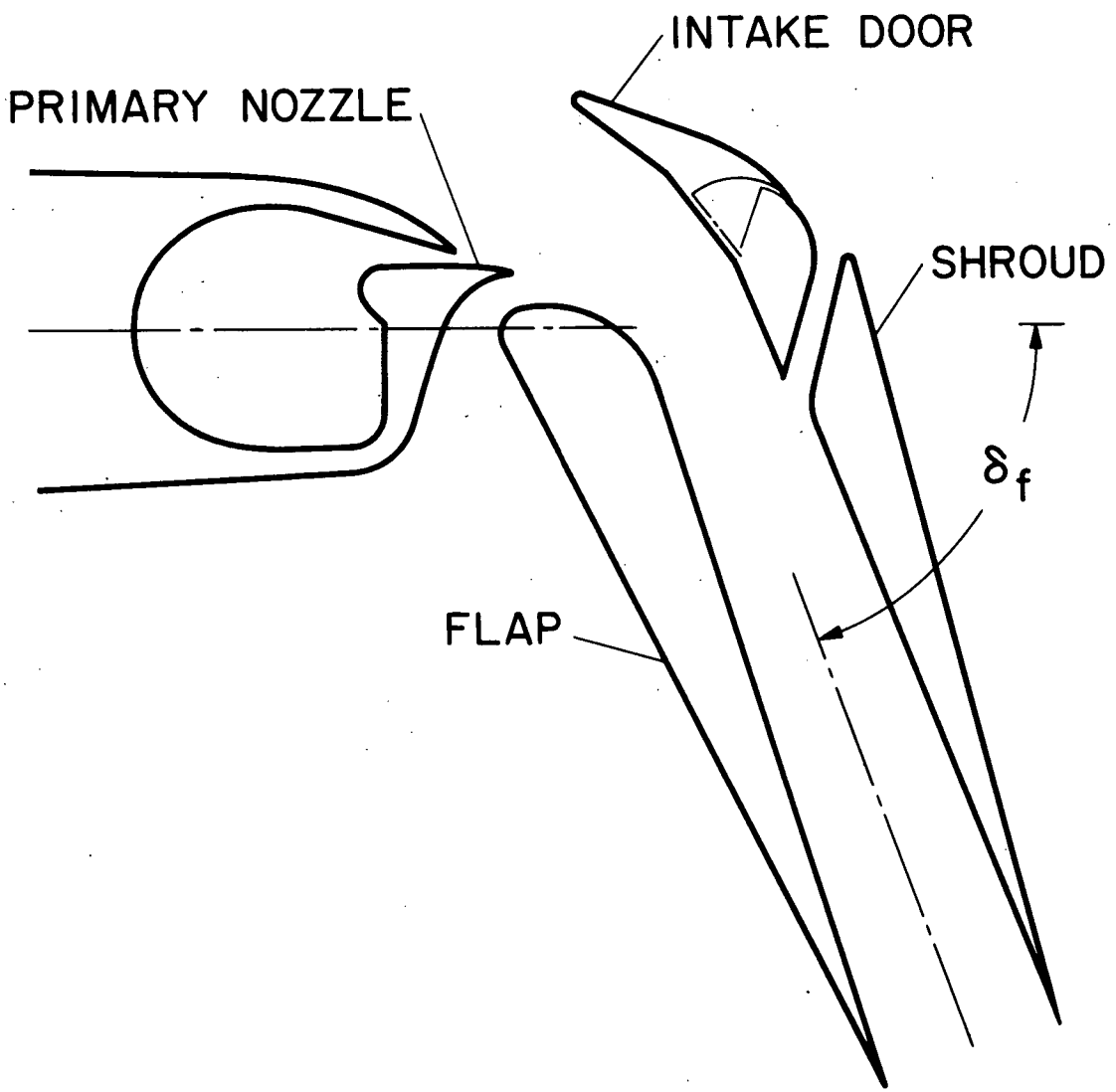

Figure 19.- Geometry of the augmentor flap.

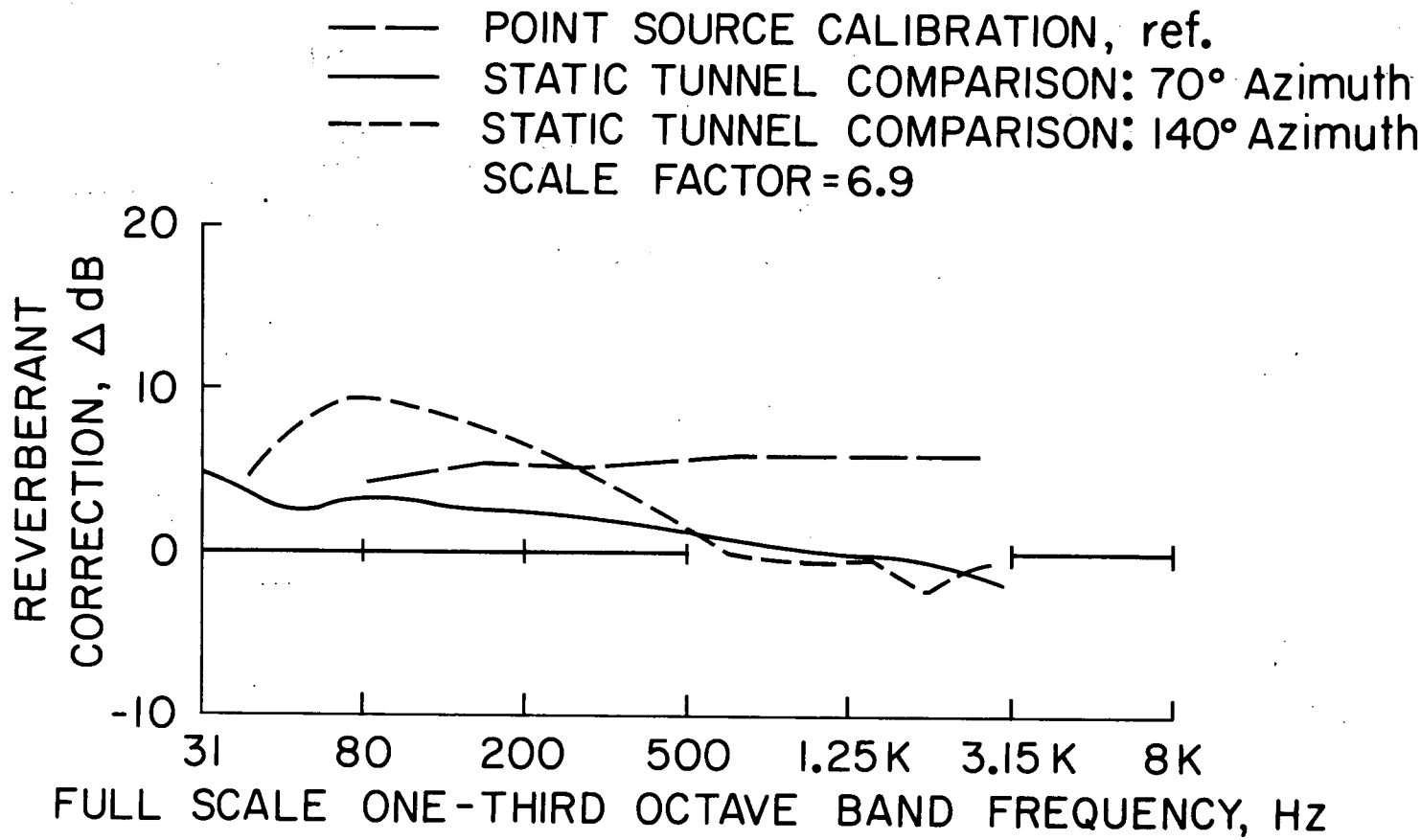

Figure 20.- Variation of reverberation with microphone position in the wind tunnel test section.

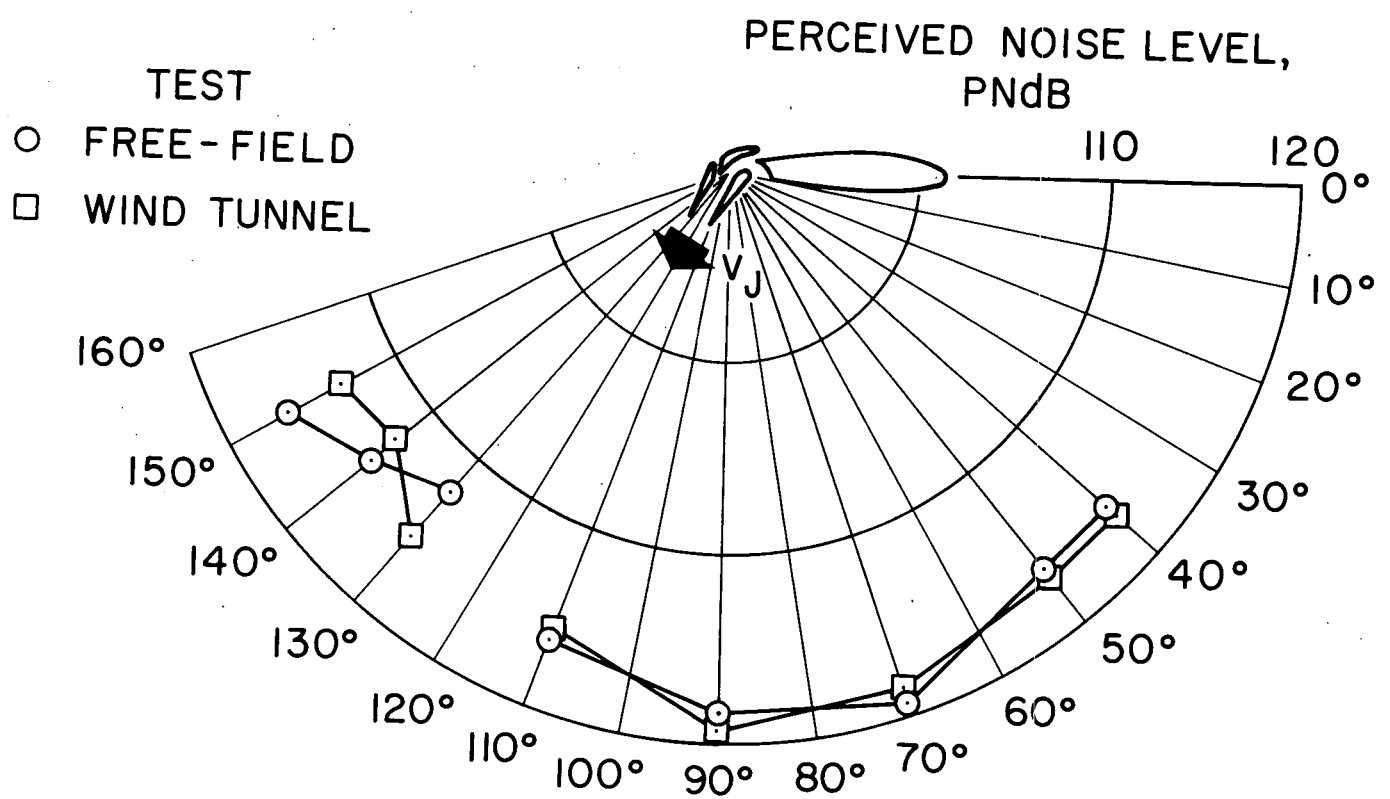

Figure 21.- Comparison of the swept augmentor wing perceived noise level directivity pattern in the free-field and the wind tunnel; q = 0 psf, PTAUG = 61 cm Hg (24 in Hg), δ_f = 60°, 152 m (500ft) full scale.

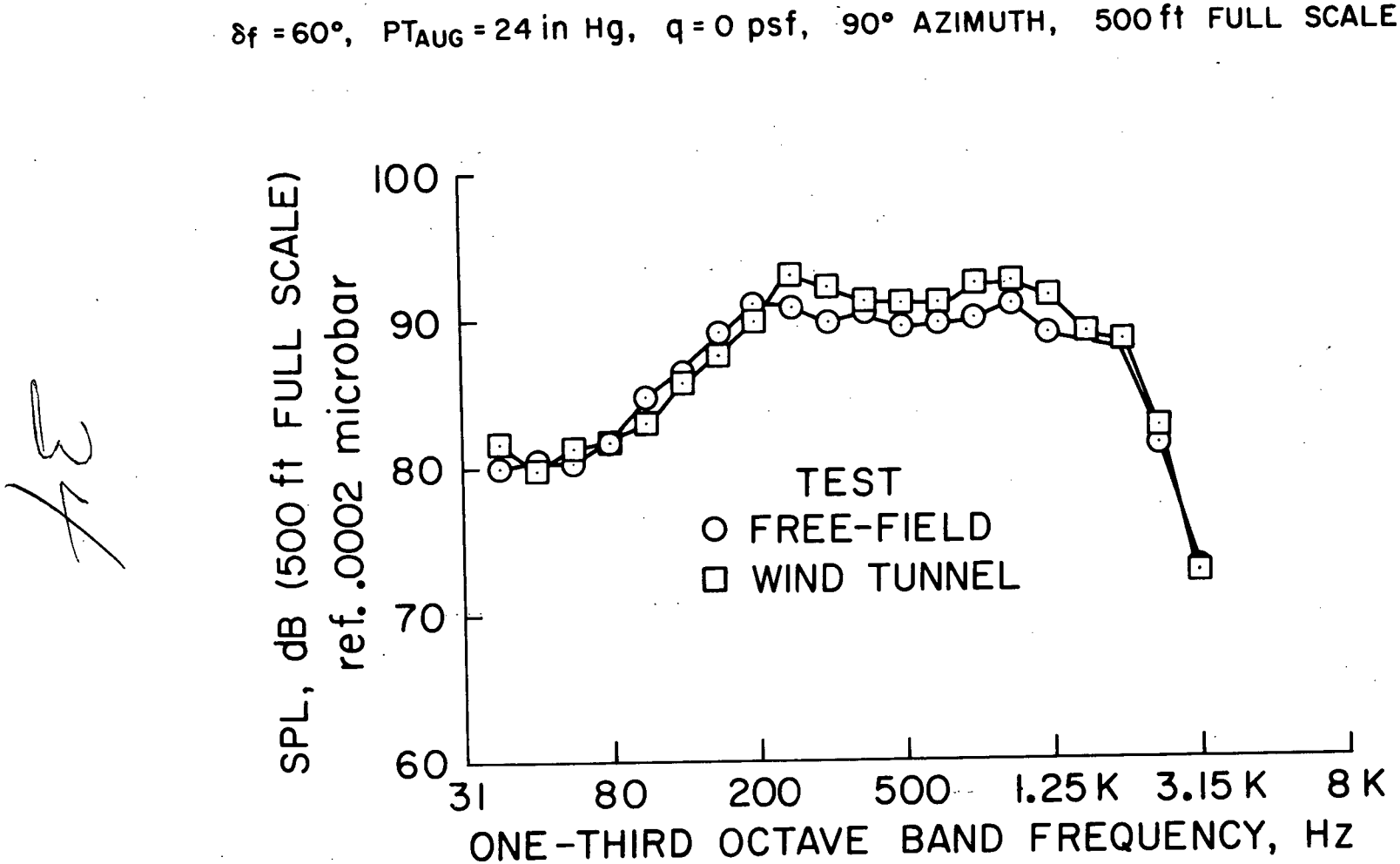

Figure 22.- Comparison of the frequency spectrum of the swept augmentor wing in the free-field and the wind tunnel; q = 0 psf, PTAUG = 61 cm Hg (24 in Hg), δ_f = 60°, 152 m (500 ft) full scale, 90° azimuth.